JOURNAL OF AGRICULTURAL AND FOOD CHEMISTRY

# Single-Bead Immunoassays Using Magnetic Microparticles and Spectral-Shifting Quantum Dots

AMIT AGRAWAL, TUSHAR SATHE, AND SHUMING NIE*

Departments of Biomedical Engineering and Chemistry, Emory University and Georgia Institute of Technology, Suite 2001, 101 Woodruff Circle, Atlanta, Georgia 30322

This paper reports a single-bead immunoassay method based on the combined use of magnetic microparticles (MMPs) for target capturing/enrichment and antibody-conjugated semiconductor quantum dots (QDs) for fluorescence detection. In comparison with organic dyes and fluorescent proteins, QDs exhibit unique optical properties such as size-tunable fluorescence emission (spectral shifting), large absorption coefficients, improved brightness, and superior photostability. Magnetic beads, composed of iron oxide nanoparticles embedded in polymeric matrices, provide a platform for rapid capturing and enrichment of biomolecules and pathogens in dilute biological and environmental samples. However, a major problem in using magnetic beads for fluorescence immunoassays is that the bead's autofluorescence strongly interferes with the target detection signal. This spectral overlapping problem can be overcome by using semiconductor QDs as a new class of spectral-shifting labels. By shifting the QD emission signals away from the bead autofluorescence, it is possible to detect biomolecular antigens such as tumor necrosis factor (TNF-α) at femtomolar ($10^{-15}$ M) concentrations when the target molecules are captured and enriched on the magnetic bead surface. This sensitivity is almost 1000 times higher that that of traditional immunoabsorbent assays and more than 100 times higher than immunofluorescent assays using organic dyes.

**KEYWORDS: Immunoassay; quantum dot; nanoparticles; sandwich assay; fluorescence**

## INTRODUCTION

Immunoassays using fluorophore-labeled antibodies are a popular technique for the detection and screening of biological molecules, cells, and pathogens (*1*, *2*). These assays are often carried out in a sandwich format in which two antibodies simultaneously recognize two binding sites on the same target molecule. This two-site sandwich method relies on a "double-selection" process to improve both detection sensitivity and specificity, and the target molecules do not need to be chemically modified or derivatized. However, these promising features are limited by the less than optimal absorption and emission properties of traditional organic dyes such as low signal intensity, rapid photobleaching, and broad emission spectra. Recent advances in nanotechnology have led to a new class of biological detection labels based on semiconductor quantum dots (QDs) for a broad range of applications, including single-molecule biophysics, biomolecular profiling, optical barcoding, and in vivo imaging (*3*−*7*). Quantum dots have unique optical and electronic properties such as size-tunable light emission, improved signal brightness, resistance against photobleaching, and simultaneous excitation of multiple fluorescence colors. Surface-passivated QDs are highly stable against photobleaching and have narrow, symmetrical emission peaks [as narrow as 14 nm full width at half-maximum (fwhm)]. It has been estimated that CdSe QDs are about 10−100 times brighter (depending on the particle size and quantum yields) and are more than 1000 times more stable against photobleaching than organic dyes. These properties have made QDs an ideal label for ultrasensitive, multiplexed, and quantitative immunoassays with broad applications in biological, agricultural, and food chemistry.

Here we report the use of magnetic microbeads and fluorescent QDs for advanced immunochemical analysis. These magnetic beads are composed of iron oxide nanoparticles embedded in a polymeric matrix and are well suited for target capturing, enrichment, and isolation (*8*−*10*). They are also being used for isolating foodborne bacteria (*11*, *12*) and for removing environmental toxins such as heavy metals and chemical waste (*13*, *14*). In particular, we have developed magnetic/optical bead-based immunoassays to detect secreted antigens such as tumor necrosis factor α (TNF-α). As an essential mediator of inflammatory and immunodefense functions, TNF-α is a polypeptide cytokine that is produced by macrophages and other cells in response to bacterial infection, injury, and inflammation (*15*, *16*). Elevated levels of TNF-α have been associated with several pathological states (*15*, *17*), whereas it is present in only trace amounts in the serum of healthy individuals. Several food products contain proteins (*18*) or contaminants (e.g., trichothecene vomitoxin in wheat and corn supplies) (*19*) that may

* Author to whom correspondence should be addressed [telephone (404) 712-8595; fax (404) 727-9873; e-mail snie@emory.edu].

10.1021/jf0635006 CCC: $37.00 © 2007 American Chemical Society
Published on Web 04/25/2007

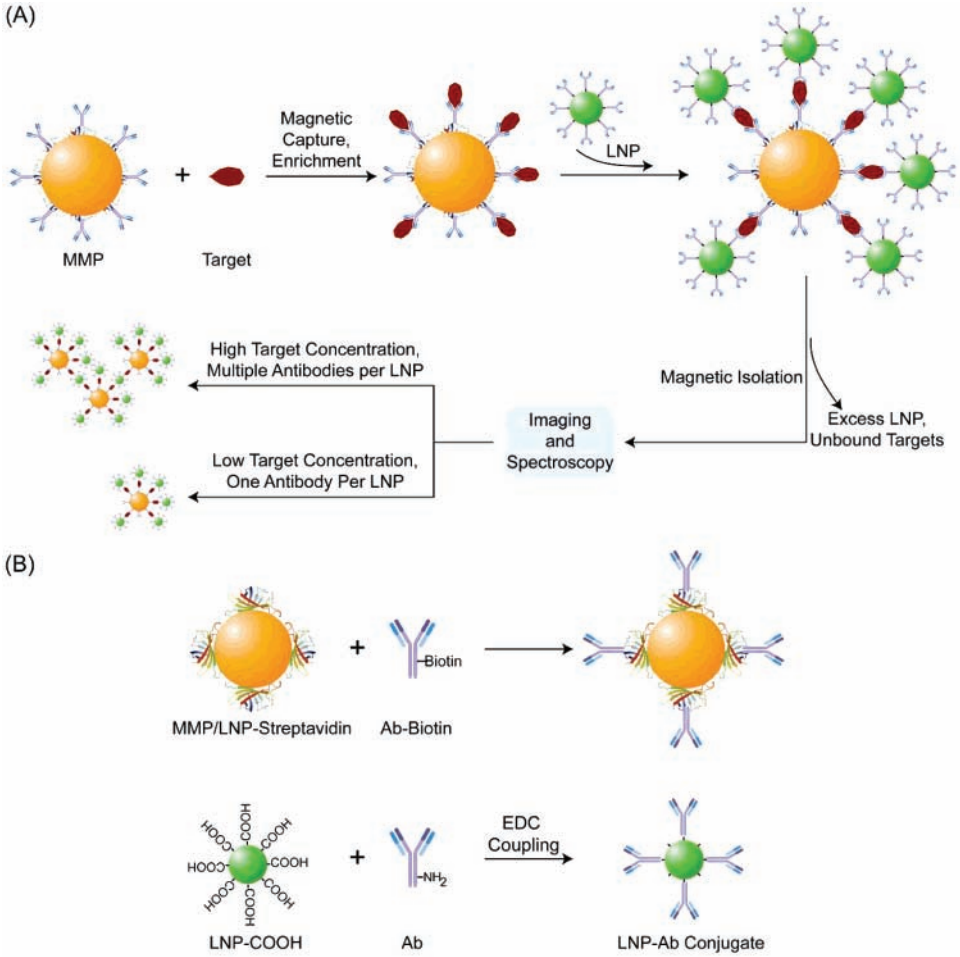


**Figure 1.** Schematic illustration of magnetic/optical bead immunoassays. (**A**) Antibody-conjugated magnetic microparticles (MMPs) capture and enrich target molecules in a dilute sample solution. After washing, the capture target molecules are detected by using bioconjugated labeling nanoparticles (LNP) such as quantum dots in a sandwich-binding format. Single beads are analyzed by wavelength-resolved spectroscopy and fluorescence imaging on an optical microscope. (**B**) Two conjugation schemes are based on non-covalent streptavidin–biotin binding and covalent carboxylate–primary amine coupling, respectively.

trigger TNF-α release in the host. A number of food allergens (e.g., cow's milk) are also known to increase the secretion level of TNF-α (*20*, *21*). Due to its biological significance, it is important to develop more rapid and sensitive assays for TNF-α detection (*22*, *23*), especially in highly dilute biological samples for screening of potential allergens in various food products.

## EXPERIMENTAL METHODS

**Bioconjugation.** Streptavidin-coated MMPs (2.8 μm diameter, 6.7 million beads; Invitrogen Inc., Carlsbad, CA) were first washed with a blocking solution (BlockAid, Invitrogen Inc.) and then mixed with biotinylated monoclonal murine TNF-α antibody (0.5 mg/mL T9160-14d, 20 μL, U.S. Biologicals Inc., Swampscott, MA) in PBS buffer (10 mM, pH 7.4, Sigma-Aldrich, St. Louis, MO). After 30 min at room temperature, the MMPs were purified by applying a 1.5 T magnetic field using a permanent magnet (Sintered Neodymium Iron Boron Magnet, MCE Magnets Inc., Torrance, CA) and were washed three times with the PBS buffer to remove unbound antibody molecules. An excess of free avidin (Sigma-Aldrich Inc.) was added to the purified constructs to saturate all free biotin binding sites. For QD bioconjugation, 10 nM streptavidin-coated QDs with emission at 525 or 605 nm (Invitrogen Inc.) were conjugated with biotinylated monoclonal antibody for murine TNF-α (333 μM MP6-XT3, BD Pharmingen Inc., San Jose, CA) in PBS buffer (10 mM, pH 7.4, Sigma-Aldrich Inc.). The antibodies were selected to ensure simultaneous binding to the target molecule. QD probes were also incubated with excess of free avidin molecules to saturate all free biotin sites on the antibody. Tetramethylrhodamine and biotin-labeled dextran (Invitrogen Inc.) were also used to test the detection limit using identical experimental procedures.

Carboxylate-modified yellow/green FluoSpheres (F8795, excitation/emission 505/515, 43 nm diameter, Invitrogen Inc.) were conjugated to monoclonal murine TNF-α antibody (T9160-16A, 1 mg/mL, U.S. Biologicals Inc.) using an aqueous-based 1-ethyl-3-(3-dimethylaminopropyl)carbodiimide hydrochloride (EDC; Sigma-Aldrich) coupling reaction (*24*). Specifically, 5 μL of the FluoSphere stock solution was added to 40 μL of 25 mM MES buffer (pH 5.9), and the mixture was sonicated for 15 min. Next, the EDC solution at a concentration of 5 mg/mL (20 μL, 100 μg total) was added to the bead solution and was vortexed for 15 min. Similarly, 11 μL of *N*-hydroxysulfosuccinimide (sulfo-NHS; Thermo-Fisher Scientific, Rockford, IL) at 14 mg/mL concentration was added to the bead solution and was vortexed for 15 min. Thereafter, 2.5 μL of TNF-α antibody at a stock concentration of 1 mg/mL was added to the solution and vortexed for 1 h. Next, 100 μg of EDC (as freshly prepared solution in MES buffer) was added, and the solution was vortexed for 75 min (total reaction volume was 100 μL). Finally, the reaction product was filtered by using an S-400 HR size exclusion filtration column (GE Healthcare, Piscataway, NJ) to remove unreacted antibody molecules.

**Antibody−Antigen Binding.** One microliter of magnetic microparticle (MMP)−antibody conjugates was mixed with recombinant murine TNF-α molecule (R&D Systems Inc., Minneapolis, MN) in various concentrations (from $6 \times 10^{-9}$ to $10^{-17}$ M) in 1 mL of PBS buffer (10 mM PBS, pH 7.4 + 0.1% BSA + 0.02% sodium azide + 0.02% Tween 20) and was allowed to react with vigorous stirring at

room temperature for 2 h. The MMPs were pulled down using a 1.5 T magnet (Sintered Neodymium Iron Boron Magnet, MCE Magnets Inc.) and were washed three times with the PBS buffer. The MMPs with TNF-α molecules captured on their surfaces were resuspended in 90 μL of PBS buffer and were allowed to react with 10 μL of Fluosphere−antibody conjugate with vigorous vortexing for 1 h at room temperature. Finally, the reaction product was pulled down using magnet, washed two times with the PBS buffer, and concentrated to 10 μL before imaging. Similar protocols were used to label TNF-α with QD−antibody conjugates.

**Data Acquisition and Analysis.** All images were taken using an Olympus IX-71 microscope (Center Valley, PA) that was equipped with a mercury lamp for excitation, a Nikon D70 color digital camera, and a 100× objective (NA 1.25, oil). The hybridized or control sample (~1−3 μL) was spread between two clean cover slips (no. 1 coverglass, Corning Inc., Acton, MA) and was placed on an epi-fluorescence microscope. True color fluorescence images were obtained by using 488-nm excitation and a long pass filter (505 nm, Chroma Technology Corp., Brattleboro, VT). The exposure times were 0.2−2 s. The fluorescence spectra of the QDs and the fluospheres ($\lambda_{ex}$ = 505 nm, $\lambda_{em}$ = 515 nm; Invitrogen Inc.) were recorded by using a standard fluorometer (FluoMax; Jobin Yvon, Edison, NJ), and the spectra of single MMPs were recorded by using a spectrophotometer (SpectraPro 150, Roper Scientific, Trenton, NJ) attached to the side port of the microscope. All images were analyzed by using NIH Image J software (*25*).

## RESULTS AND DISCUSSION

The basic principles of our magneto-optical immunoassays are shown in **Figure 1**. In this scheme, magnetically responsive microbeads or microparticles (MMP) are coated with a monoclonal capture antibody that is specific for the target molecule. After the target molecules are captured on the bead, a magnetic field is applied to isolate these beads. Following target capturing and enrichment, fluorescent nanoparticle probes conjugated with another monoclonal antibody are used to label the target in a "sandwich" format. Free or unbound QD probes are removed by washing in the presence of the magnetic field. The QD-labeled magnetic beads are then placed on a thin glass coverslip for spectroscopic measurement and imaging using a fluorescence microscope. It is important to note that the sandwich format eliminates the need for direct target tagging, a task that is often inefficient and time-consuming for low-concentration samples. It also minimizes sample handling and ensures the safety of workers dealing with samples that may be contaminated with infectious agents.

To evaluate the detection sensitivity of our bead-based assays, we have used a biotinylated dextran−dye conjugate [dextran conjugated to tetramethylrhodamine (TMR) and biotin] (Invitrogen Inc.) to streptavidin-coated magnetic microbeads. High-resolution fluorescence images are obtained from single beads at various dextran−dye concentrations (**Figure 2**, top). The integrated fluorescence intensities are also measured and plotted as a function of dextran−dye concentration (**Figure 2**, bottom). The results indicate that 1 pM ($10^{-12}$ M) dextran−dye conjugate yields a detectable signal above the bead autofluorescence background, but below this value, the dextran−dye signals are buried under the bead autofluorescence and cannot be detected reliably.

To further examine how this autofluorescence interferes with the QD signals, we have obtained and compared the emission spectra of magnetic microbeads with those of QD-605, QD-525, and dye-embedded nanoparticles (**Figure 3**). When a blue excitation source is used ($\lambda_{ex}$ ~ 488 nm), there is indeed significant spectral overlap between the MMP emission and the QD-605. However, the spectral overlap is significantly reduced

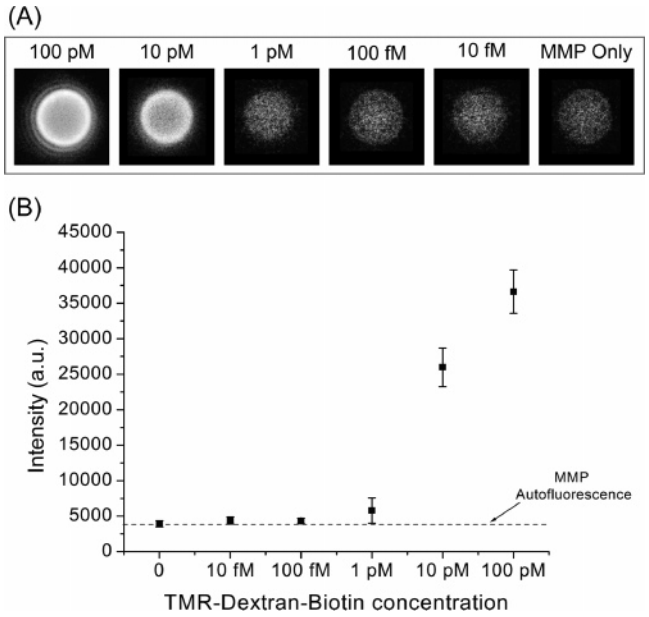


**Figure 2.** Single-bead immunoassay and quantitative analysis of bead signal intensities as a function of dye label concentration: (**A**) fluorescence images of single magnetic microparticles (MMPs) after incubation with different concentrations of a dextran–dye label; (**B**) plot of the integrated bead fluorescence intensity as a function of concentration of the dye–dextran conjugate (error bars show the standard deviation for sample sizes >5). The average background signal outside each bead was subtracted to obtain the fluorescent signal from the bead.

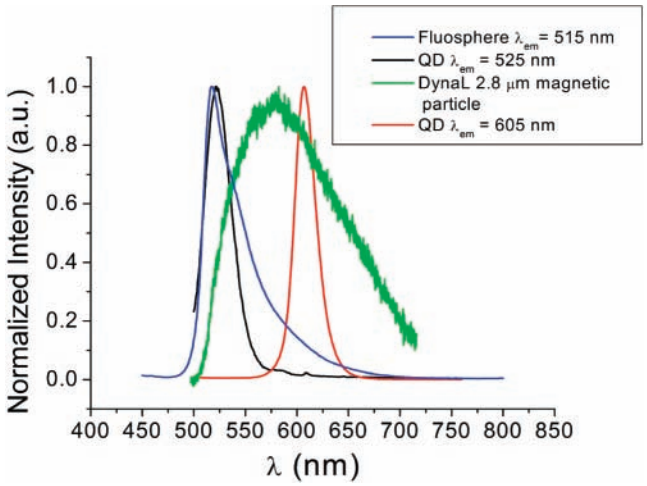


**Figure 3.** Comparison of fluorescence emission spectra among magnetic microbeads, quantum dots, and dye-embedded nanoparticles. Note that MMP emission has significant overlap with QD605 emission, but this overlap is greatly reduced when the QD emission spectrum is shifted to 525 nm.

when the QD emission spectrum is shifted to 525 nm. Due to the unique excitation profiles of semiconductor QDs, a blue light source can be used to excite multicolored QDs, leading to Stokes wavelength shifts as large as 300−350 nm. This novel feature becomes critically important when complex materials such as polymer beads embedded with magnetic nanoparticles and "real-world" biological samples that often exhibit high background fluorescence across a broad wavelength range are examined. In comparison, organic dyes and fluorescent proteins give rise to small Stokes shifts, and their emission signals are often in the same spectral region as background fluorescence.

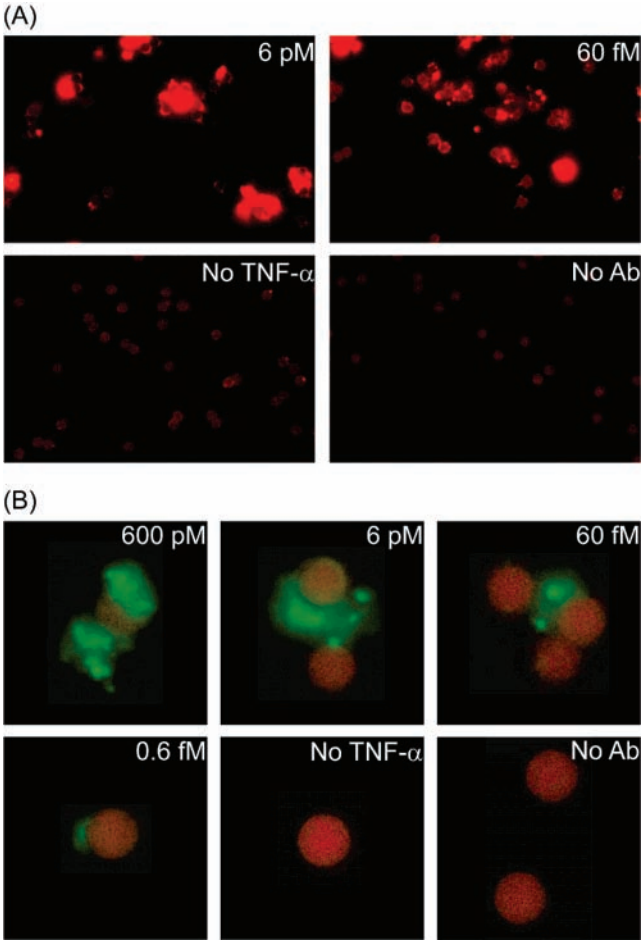


**Figure 4.** Bead-based immunoassay of tumor necrosis factor α (TNF) using magnetic microbeads for capturing and spectral-shifiting QDs for labeling: (**A**) fluorescence images of magnetic beads obtained by using QD-605 probes at various TNF concentrations and control conditions, showing color overlap between the bead autofluorescence and the QD emission; (**B**) fluorescence images of magnetic beads obtained by using QD-525 probes at various TNF concentrations and control conditions, showing a spectral shift of the QD signal away from the bead autofluorescence background. See text for detailed discussion.

To take advantage of this spectral-shifting effect, we prepared QD−antibody probes for labeling TNF-α protein molecules captured on the MMP probes. As shown in **Figure 4**, the use of green-emitting QD probes (but not red-emitting dots) allows a clear differentiation from the bead autofluorescence (orange). A further interesting observation is that QD probes with excess monoclonal antibodies lead to MMP aggregation when the TNF-α concentration is increased (**Figure 4A**). This type of bead aggregation is similar to the phenomenon of "latex agglutination" because the QD probes often have multiple binding sites. Thus, a single QD probe could simultaneously bind to two or more magnetic beads, leading to multivalent binding and aggregation (see **Figure 1**). As shown by the control studies, bead aggregation is not observed in the absence of TNF-α (no TNF-α) or without antibody conjugation to QDs (no Ab). Using green-emitting QD probes (QD-525), target TNF-α signals can be detected at concentrations as low as 1 fM ($1 \times 10^{-15}$ M). At such low concentrations, the probabilities of multivalent QD binding are very small and bead aggregation is reduced. In control experiments in which no TNF-α was used or the particles were not coupled with antibodies, no QD-525 signal was seen on the magnetic beads. These results suggest

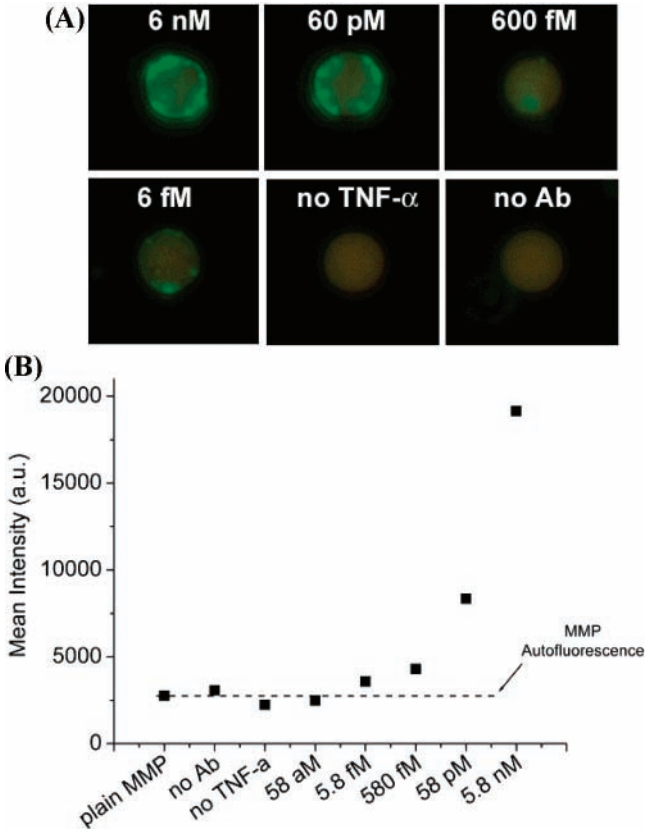


**Figure 5.** Bead-based immunoassay of tumor necrosis factor α (TNF) using magnetic microbeads for capturing and dye-embedded nanoparticles for labeling: (**A**) fluorescence images of single beads obtained at various TNF concentrations and control conditions; (**B**) plot of the integrated bead fluorescence intensity as a function of TNF concentration. The average background signal outside each bead was subtracted to obtain the fluorescent signal from the bead.

that the immunoassay detection sensitivities achieved with spectral-shifting QDs are 2−3 orders of magnitude higher than that with organic dyes.

We have further investigated whether other classes of fluorescent nanoparticle probes could be used with magnetic microbeads. In particular, dye-embedded polymer nanoparticles are bright and photostable and offer advantages similar to those of QD probes. **Figure 5** shows the results for TNF-α labeling and detection obtained with 515-nm emitting dye-doped nanoparticles (43-nm diameter). Green fluorescence from the nanoparticle labels can be detected at TNF-α concentrations as low as 6 fM, but no signal is seen in the absence of TNF-α or antibody. To determine the detection sensitivity more quantitatively, the integrated bead fluorescence is calculated and is plotted as a function of TNF-α concentration (**Figure 5B**). This analysis confirms that the target signals obtained at 6 fM concentration are well above the background level. Further studies are still needed to examine the dynamic range and linearity of this single-bead assay method.

A potential limiting factor is that antibody−antigen interactions have finite dissociation equilibrium constants ($k$), on the order of $10^{-9}$−$10^{-12}$ M. Using second-order binding kinetics as a first approximation, an excess probe concentration equal to $k$ leads to 50% target binding at equilibrium. To achieve 90% target binding, the excess probe concentration must be 9$k$. This simple analysis suggests that significant probe excess is needed to drive protein binding. On the other hand, excess probes will cause more background noise and could interfere with measure-

ment. On the basis of the level of nonspecific background signals with cytokine antibodies, we estimate that the maximum probe concentrations could be increased to about 10−20 times the equilibrium constant $k$ to achieve 90−95% target binding. An alternative approach is to mix the probes and targets at high concentrations and then dilute the mixture immediately prior to analysis. In this case, the stability of the complex becomes an important factor. Recent work by Klenerman et al. (*26*) has found that the dissociation rates for the IgG antibody−antigen complex are ca. $3 \times 10^3\ s^{-1}$ and that the dissociation equilibrium constants for the antigen−antibody dimer $Ag-Ab_2$ are ca. $2.3 \times 10^{-21}\ M^2$. Under these conditions, quantitative measurement of protein−antibody complexes were reported over 3 orders of magnitude, and the achieved sensitivity was found to be limited by the slow rate for target molecules to encounter the probe laser beam.

In conclusion, we have reported a combined magnetic enrichment and optical detection method for ultrasensitive immunoassays of secreted proteins in dilute samples. In this method, magnetic microbeads are used for efficient target capturing and antibody-conjugated semiconductor quantum dots for fluorescence labeling. A key finding is that by shifting the QD emission signals away from the bead autofluorescence, it is possible to detect biomolecular antigens such as tumor necrosis factor (TNF-α) at concentrations as low as 1−10 fM [$(1-10) \times 10^{-15}$ M). This sensitivity is about 2−3 orders of magnitude higher than that achieved with current immunoassay methods. By using differently colored QDs conjugated to different antibodies (each recognizing a specific antigen), we envision that multiplexed bead assays can be developed to detect a panel of biological molecules and pathogens in food, agricultural, and environmental samples.

## LITERATURE CITED


(1) Sheikh, S. H.; Abela, B. A.; Mulchandani, A. Development of a fluorescence immunoassay for measurement of paclitaxel in human plasma. *Anal. Biochem.* **2000**, *283* (1), 33−38.

(2) Hicks, J. M. Fluorescence immunoassay. *Hum. Pathol.* **1984**, *15* (2), 112−116.

(3) Chan, W. C.; Nie, S. Quantum dot bioconjugates for ultrasensitive nonisotopic detection. *Science* **1998**, *281* (5385), 2016−2018.

(4) Reck-Peterson, S. L.; Yildiz, A.; Carter, A. P.; Gennerich, A.; Zhang, N.; Vale, R. D. Single-molecule analysis of dynein processivity and stepping behavior. *Cell* **2006**, *126* (2), 335−348.

(5) Han, M.; Gao, X.; Su, J. Z.; Nie, S. Quantum-dot-tagged microbeads for multiplexed optical coding of biomolecules. *Nat. Biotechnol.* **2001**, *19* (7), 631−635.

(6) Gao, X.; Cui, Y.; Levenson, R. M.; Chung, L. W.; Nie, S. In vivo cancer targeting and imaging with semiconductor quantum dots. *Nat. Biotechnol.* **2004**, *22* (8), 969−976.

(7) Agrawal, A.; Zhang, C.; Byassee, T.; Tripp, R. A.; Nie, S. Counting single native biomolecules and intact viruses with color-coded nanoparticles. *Anal. Chem.* **2006**, *78*, 1061−1070.

(8) Ahmed, A. R.; Olivier, G. W.; Adams, G.; Erskine, M. E.; Kinsman, R. G.; Branch, S. K.; Moss, S. H.; Notarianni, L. J.; Pouton, C. W. Isolation and partial purification of a melanocyte-stimulating hormone receptor from B16 murine melanoma cells. A novel approach using a cleavable biotinylated photoactivated ligand and streptavidin-coated magnetic beads. *Biochem. J.* **1992**, *286* (Part 2), 377−382.

(9) Xu, H.; Sha, M. Y.; Wong, E. Y.; Uphoff, J.; Xu, Y.; Treadway, J. A.; Truong, A.; O'Brien, E.; Asquith, S.; Stubbins, M.; Spurr, N. K.; Lai, E. H.; Mahoney, W. Multiplexed SNP genotyping using the Qbead system: a quantum dot-encoded microsphere-based assay. *Nucleic Acids Res.* **2003**, *31* (8), e43.

(10) Ossendorp, F. A.; Bruning, P. F.; Van den Brink, J. A.; De Boer, M. Efficient selection of high-affinity B cell hybridomas using antigen-coated magnetic beads. *J. Immunol. Methods* **1989**, *120* (2), 191−200.

(11) Yitzhaki, S.; Zahavy, E.; Oron, C.; Fisher, M.; Keysary, A. Concentration of *Bacillus* spores by using silica magnetic particles. *Anal. Chem.* **2006**, *78*, 6670−6673.

(12) Yang, L.; Li, Y. Simultaneous detection of *Escherichia coli* O157:H7 and *Salmonella typhimurium* using quantum dots as fluorescence labels. *Analyst* **2006**, *131* (3), 394−401.

(13) Ngomsik, A. F.; Bee, A.; Siaugue, J. M.; Cabuil, V.; Cote, G. Nickel adsorption by magnetic alginate microcapsules containing an extractant. *Water Res.* **2006**, *40* (9), 1848−1856.

(14) Rorrer, G. L.; Hsien, T. Y.; Way, J. D. Synthesis of porous-magnetic chitosan beads for removal of cadmium ions from wastewater. *Ind. Eng. Chem. Res.* **1993**, *32*, 2170−2178.

(15) Tracey, K. J.; Cerami, A. Tumor necrosis factor: a pleiotropic cytokine and therapeutic target. *Annu. Rev. Med.* **1994**, *45*, 491−503.

(16) Beutler, B.; Cerami, A. Tumor necrosis, cachexia, shock, and inflammation: a common mediator. *Annu. Rev. Biochem.* **1988**, *57*, 505−518.

(17) de Kossodo, S.; Houba, V.; Grau, G. E. Assaying, tumor necrosis factor concentrations in human serum. A WHO International Collaborative study. *J. Immunol. Methods* **1995**, *182* (1), 107−114.

(18) Simuth, J.; Bilikova, K.; Kovacova, E.; Kuzmova, Z.; Schroder, W. Immunochemical approach to detection of adulteration in honey: physiologically active royal jelly protein stimulating TNF-α release is a regular component of honey. *J. Agric. Food Chem.* **2004**, *52*, 2154−2158.

(19) Wong, S. S.; Zhou, H. R.; Marin-Martinez, M. L.; Brooks, K.; Pestka, J. J. Modulation of IL-1$\beta$, IL-6 and TNF-α secretion and mRNA expression by the trichothecene vomitoxin in the RAW 264.7 murine macrophage cell line. *Food Chem. Toxicol.* **1998**, *36* (5), 409−419.

(20) Heyman, M.; Darmon, N.; Dupont, C.; Dugas, B.; Hirribaren, A.; Blaton, M. A.; Desjeux, J. F. Mononuclear cells from infants allergic to cow's milk secrete tumor necrosis factor α, altering intestinal function. *Gastroenterology* **1994**, *106* (6), 1514−1523.

(21) Majamaa, H.; Miettinen, A.; Laine, S.; Isolauri, E. Intestinal inflammation in children with atopic eczema: faecal eosinophil cationic protein and tumour necrosis factor-α as non-invasive indicators of food allergy. *Clin. Exp. Allergy* **1996**, *26* (2), 181−187.

(22) Nowak-Wegrzyn, A. Future approaches to food allergy. *Pediatrics* **2003**, *111* (6 Part 3), 1672−1680.

(23) Wang, J.; Liu, G.; Engelhard, M. H.; Lin, Y. Sensitive immunoassay of a biomarker tumor necrosis factor-α based on poly(guanine)-functionalized silica nanoparticle label. *Anal. Chem.* **2006**, *78*, 6974−6979.

(24) Hermanson, G. T. *Bioconjugate Techniques*; Academic Press: San Diego, CA, 1996; pp xxv, 173-176, 785.

(25) Rasband, W. S. Image J. Oct 15, 2006.

(26) Li, H.; Zhou, D.; Browne, H.; Balasubramanian, S.; Klenerman, D. Molecule by molecule direct and quantitative counting of antibody−protein complexes in solution. *Anal. Chem.* **2004**, *76*, 4446−4451.


**Received for review December 4, 2006. Revised manuscript received February 16, 2007. Accepted March 9, 2007. This work was supported in part by NIH grants (P20 GM072069, R01 CA108468-01, and U54CA119338) and the Georgia Cancer Coalition Distinguished Cancer Scholars Program (to S.N.).**

JF0635006